Wireless Pers Commun
DOI 10.1007/s11277-011-0242-6

Integrated Common Radio Resource Management with Spectrum Aggregation Over Non-Contiguous Frequency Bands

O. Cabral · F. Meucci · A. Mihovska · F. J. Velez · N. R. Prasad · R. Prasad

Abstract This paper proposes an Integrated Common Radio Resource Management (iCRRM). The iCRRM performs classic CRRM functionalities jointly with Spectrum Aggregation (SA), being able to switch users between non-contiguous frequency bands. The SA scheduling is obtained with an optimised General Multi-Band Scheduling algorithm with the aim of cell throughput maximisation. In particular, we investigate the dependence of the throughput on the cell coverage distance for the allocation of users over the 2 and 5 GHz bands for a single operator scenario under a constant average Signal to Interference-plus-Noise Ratio. For the performed evaluation, the same type of Radio Access Technology is considered for both frequency bands. The operator has the availability of a non-shared 2 GHz band and has access to part (or all) of a shared frequency band at 5 GHz. The performance gain, analysed in terms of data throughput, depends on the channel quality for each user in the considered bands which, in turn, is a function of the path loss, interference, noise, and the distance from the Base Station. An almost constant gain near 30% was obtained with the proposed optimal solution compared to a system where users are first allocated in one of the two bands and later not able to handover between the bands.

O. Cabral (✉) · F. J. Velez
Instituto de Telecomunicações, DEM, Universidade da Beira Interior, Covilhã, Portugal
e-mail: orlandoc@ubi.pt

F. J. Velez
e-mail: fjv@ubi.pt

F. Meucci
Electronics and Telecommunication Department, Università di Firenze, Florence, Italy
e-mail: filippo.meucci@unifi.it

O. Cabral · F. Meucci · A. Mihovska · N. R. Prasad · R. Prasad
Center for TeleInFrastruktur (CTIF), Aalborg University, Aalborg, Denmark

A. Mihovska
e-mail: albena@es.aau.dk

N. R. Prasad
e-mail: np@es.aau.dk

R. Prasad
e-mail: prasad@es.aau.dk

Published online: 22 February 2011

Keywords Wireless systems · Radio resource management · Spectrum aggregation · SINR

Abbreviations

AC	Allocation Constraint
ACK	Acknowledgement
AMC	Adaptive Modulation and Coding
BC	Bandwidth Constraint
BS	Base Station
CA	Carrier Aggregation
CPICH	Common Pilot Channel
CQI	Channel Quality Indicator
CRRM	Common RRM
DL	Downlink
GAP	General Assignment Problem
GMBS	General Multi-Band Scheduling
H-ARQ	Hybrid Automatic Repeat Request
HSDPA	High Speed Downlink Packet Access
HS-DPCCS	High-Speed Dedicated Physical Control Channel
IMT-A	International Mobile Telecommunications-Advanced
IP	Integer Programming
LTE	Long Term Evolution
LTE-A	Long Term Evolution-Advanced
MBS	Multi-Band Scheduling
MCS	Modulation and Coding Scheme
MO-GAP	Multiple Objectives GAP
MPDU	MAC Packet Data Unit
MS	Mobile Station
NRTV	Near Real Time Video
PER	Packet Error Rate
PF	Profit Function
PHY	Physical Layer
QoE	Quality of Experience
QoS	Quality of Service
RA	Resource Allocation
RAN	Radio Access Network
RNC	Radio Network Controller
RR	Round Robin
RRM	Radio Resource Management
SA	Spectrum Aggregation
SINR	Signal to Interference-plus-Noise Ratio
SIR	Signal-to-Interference Ratio
SO-GAP	Single Objective General Assignment Problem
ST	Service Throughput
TTI	Time Transmission Interval
WCDMA	Wideband Code Division Multiple Access
iCRRM	Integrated CRRM

1 Introduction

A key challenge for International Mobile Telecommunications-Advanced (IMT-A) infrastructures is the ability to operate in the preferred frequency bands, as announced in WRC-07 [1], while maximising network performance and maintaining intra-systems compatibility. The current problem of spectrum fragmentation requires a different approach to enable the bandwidth required by IMT-A systems. Spectrum and Carrier Aggregation are two enabling techniques proposed for Long Term Evolution-Advanced (LTE-A) [2] and IMT-A [3,4] for achieving the advanced technical requirements identified for those systems. The physical layer aspects of LTE-A have been discussed in [5–7].

Spectrum Aggregation (SA) consists in aggregating several (and possibly) fragmented bands. The concept of spectrum aggregation consists of exploiting multiple small spectrum fragments simultaneously (aggregation) to yield to a (virtual) single larger band and ultimately deliver a wider band service (i.e., not otherwise achievable when using a single spectrum fragment). Further, SA allows that new high data rate wireless communication systems can coexist while reusing the spectrum of legacy systems.

There are two possible scenarios for SA: aggregation of contiguous bands and aggregation of non-contiguous bands. The non-contiguous approach may provide larger flexibility as well as diversity, but on the other hand is more difficult to achieve in integrated devices.

The possibility to benefit from SA increases the freedom and the complexity in the Radio Resource Management (RRM) strategy. Some of the key features of LTE-A, Release 9, are the simple protocol architecture and moving the network intelligence down to the Base Station (BS) level [5]. The added functionalities should enable the mobile operators to provide services in a more effective manner, as well as to improve the Quality of Experience (QoE). The proposed shared channel gives instantaneous access to high rate, the envisioned scheduler exploits the channel both in time and in frequency, and there would be a very high number of "always-on" users.

SA requires modifications, both at the Mobile Station (MS) side, namely, in the transceiver, and at the network side. For example, it has been proposed for LTE-A and IMT-A, that the BSs have the capability to autonomously manage the radio resource allocation. This requires that novel approaches to benefit from the SA feature must be defined. As a result, SA could be investigated at least from these two perspectives: at the lower layer to solve implementation issues, and at the upper layers to derive advanced resource management schemes to fully benefit from SA.

There are several SA studies that have been described in the literature [8–10] and [11]. The modelling and simulation aspects of SA in the context of LTE-A have been addressed in [8], including different scheduling strategies. A summary of the Carrier Aggregation (CA) types and the technical challenges in terms of various LTE-A system functionalities, such as control signalling, handover control, guard band settings, can be found in [9]. In [10], the authors analyse in more detail the load balancing aspects and related scheduling solutions under various traffic conditions in a LTE-A system utilizing CA. The work in [11] further extends the studies in [10] by addressing the feedback schemes needed for channel aware scheduling over multiple component carriers. The studies in [6] and [7] are the main baseline for the L1-L2 radio resource management.

The best choice of a frequency band for a mobile communications system depends on many different factors. Once the spectrum has been obtained, there is still the remaining problem of managing the shared band, which implies proper allocation mechanisms for allocating users based on the specific user requirements and radio channel quality. In general, the lower frequency bands are better suited to longer range, higher mobility, lower capacity

systems, while higher frequency bands are better suited to shorter range, lower mobility, and higher capacity systems. Therefore, for any given network the optimum frequency would vary depending on the required range, mobility and capacity [12].

The scheduling of users over multiple frequency bands can be modelled in its most general form as a General Multi-Band Scheduling (GMBS) problem [13]. A multi-band scheduler to manage the balance between the data pipe and the obtained extra source of spectrum was proposed in [14]. When the bandwidth from the shared band becomes available, the scheduler must be capable of realizing such a change in the spectrum pipe and shift some of the traffic load from the dedicated band to the shared band or vice versa. The scheduler must also be capable of further load balancing by actively monitoring the forthcoming changes in the spectrum and traffic data in order to shift the load from the shared band to dedicated one and vice- versa, if so required.

In Long Term Evolution (LTE), LTE-A and IMT-A, a key feature of the Radio Access Network (RAN) architecture is the Common RRM (CRRM) entity in charge of distributing resources for inter- and intra-system radio resource management purposes. In this way, the CRRM is the entity enabling the successful cooperation of the above mentioned systems with legacy systems (e.g., WiMAX, UMTS, GSM).

This paper investigates a non-contiguous SA from an upper layer point of view, and proposes an Integrated CRRM (iCRRM) entity where CRRM and SA functionalities are handled simultaneously, performing the scheduling via the optimal solution of a GMBS problem. The employed Resource Allocation (RA) allocates the user packets to the available radio resources in order to satisfy the user requirements, and to ensure efficient packet transport to maximise spectral efficiency. The RA, an entity within the set of RRM algorithms, is envisioned to have an inherent tuning flexibility to maximise the spectral efficiency of the system for any type of traffic QoS requirements. The RA adopted here maps packets of variable size into variable length radio blocks for transmission over the PHY layer, and the length is dependent on the channel quality. The novelties of the approach compared to the current state-of-the-art are that the proposed iCRRM enables the integration of spectrum and network resource management functionalities leading to higher performance and system capacity gains. The key to such integration is the pooling of the resources together; the integration allows for mapping the service requirements onto an available spectrum amount and translates the latter into network load. The iCRRM uses the widely separated frequency bands for achieving lower delays and jitters and higher user throughput by exploiting the channel diversity [15]. These show independent Channel Quality Indicator (CQI) over time and space, which becomes a source of diversity at the Physical (PHY) layer, with an important chance to achieve higher spectrum efficiency. Information from the network about the system state (e.g., received signal strength, transmitted power, MS velocity, etc) and used in RRM procedures such as load, admission and congestion control can successfully be combined with dynamic spectrum use and reduce the need of spectrum aggregation in some cases.

The integration of dynamic spectrum use and SA, achieved with the use of iCRRM techniques is shown to provide significant throughput gain compared to a system where the iCRRM is not used. A formulation is proposed for the average Signal to Interference-plus-Noise Ratio (SINR) that allows for setting the basic limits for the dependence of SA with multi-band scheduling on the coverage distance with an optimal solution.

This paper is organized as follows. Section 2 presents the objective of the paper and system model. Section 3 addresses the GMBS as a General Assignment Problem (GAP). Section 4 proposes a formulation to obtain the average SINR, with unitary reuse pattern as a function of the cell coverage distance. Section 5 discusses the SA results with the proposed iCRRM and Sect. 6 presents the conclusions.

2 Objective and System Model

In the context of SA, there are two or more frequency bands available for the operator. A CRRM framework is proposed in this work which facilitates the best user allocation over a set of m frequency bands, $b \in \{1, 2, \ldots, m\}$. The objective is to maximise the total network throughput. Without loss of generality, two bands are considered ($m = 2$). The operator has exclusive access to the channels in the 2 GHz band, and may access the shared frequency pool at 5 GHz.

The amount of radio resource available at 5 GHz is determined by spectrum trading (or bargaining) among all the operators that have access to the common frequency pool, Fig. 1. Since spectrum sharing mechanisms are beyond the scope of this work, it is assumed here that the operator gains access to the frequency pool with a fixed portion of the available spectrum. Once a part of the spectrum has been obtained, the operator still faces the problem of allocating users on the available bands. Depending on the capabilities at the MSs, each user may be allocated to a single frequency band or simultaneously to both frequency bands. In the latter case, MSs need to have multi-radio transceivers; here, single-transceiver MSs are considered that enable the selection of one carrier at a time.

An High Speed Downlink Packet Access (HSDPA) radio access network operating in the 2 and 5 GHz bands is simulated in a context of multi-user allocation [17]. CRRM is adopted from [18], as shown in the simulation setup in Fig. 2. It is responsible for allocating the available radio resources to the user traffic in a cost-effective manner, and includes a scheduling mechanism, link adaptation, code allocation policy, and an Hybrid Automatic Repeat Request (H-ARQ) scheme, to increase service throughput for users at the cell edge. In the considered scenario, inter-frequency handover between Wideband Code Division Multiple Access (WCDMA) carriers is possible, which is performed as in [19]. Besides all the common functionalities inherent to the CRRM entity, in this work it was given extra intelligence to the CRRM entity. By using an Integer Programming (IP) based algorithm, the inter-frequency

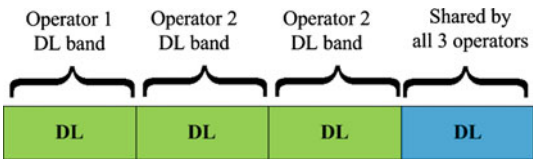

Fig. 1 Scenario of common frequency pool [16]

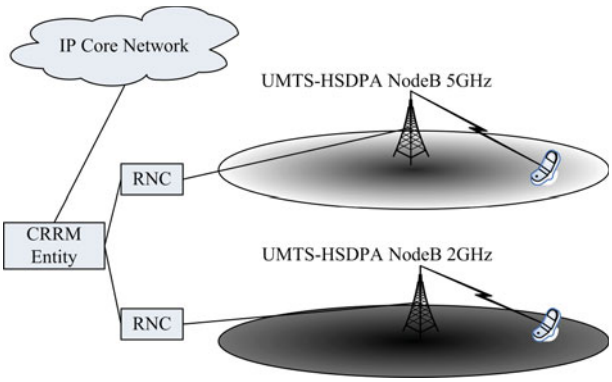

Fig. 2 CRRM in the context of SA with two separated frequency bands

handovers are performed in an optimised way, offering additional intelligence to the CRRM unit maximising system capacity.

The network is deployed with omnidirectional hexagonal cells and with frequency reuse pattern one. The results are presented only for the central cell. The session activity is modelled by the Near Real Time Video (NRTV) streaming traffic model from [20], with a service rate $S_{\text{rate}} = 64$ kbps. The RRM includes the following functionalities: Adaptive Modulation and Coding (AMC), n-parallel channel H-ARQ using chase combining and a Round Robin (RR) scheduling algorithm.

The radio channel follows the ITU radio propagation models, as summarised in Table 1. The channel loss between the MS and the BS is modelled by using a shadowing loss with log-normal distribution and by considering fast fading with Jakes model, as in [21]. The interference in the MS is calculated with the signal strength received from the first ring of neighbouring BSs and the thermal noise [22].

Each Time Transmission Interval (TTI) is associated with a sub-frame duration, that corresponds to an HSDPA frame duration of 2 ms, with three time slots of 0.67 ms. The available data rates are summarised in Table 2. The CQI is a mapping of the averages of the CQIs recorded over time; a direct mapping between CQI_{bu} and the available rate at the physical layer, in kbps, $R(\text{CQI}_{bu})$ is considered:

$$R(CQI_{bu}) = \begin{cases} 188.5 & \text{if} \quad \text{CQI}_{bu} = 5 \\ 198.0 & \text{if} \quad \text{CQI}_{bu} = 8 \\ 331.9 & \text{if} \quad \text{CQI}_{bu} = 15 \\ 716.8 & \text{if} \quad \text{CQI}_{bu} = 22 \end{cases} \tag{1}$$

where b is the band index ($b \in \{1, 2\}$) and u is the user index ($u \in \{1, 2, \ldots, n\}$, n being the number of users).

The RRM allocates the user packets to the available radio resources in order to satisfy the user requests, while ensuring efficient packet transport and maximising spectral efficiency. The RRM should have inherent tuning flexibility, to maximise the spectral efficiency of the system for any type of traffic QoS requirements. Depending on the radio channel quality, the CRRM maps data packets into variable length radio blocks, for transmission. The following events occur:

1. User packets awaiting transmission are prioritised according to the scheduling algorithm criteria;

Table 1 Parameters and models used for 2 and 5 GHz bands

Carrier frequency	2 GHz	5 GHz
Bandwidth	5 MHz	5 MHz
Path loss model (dBW)	$128.1+37.6 \cdot \log(d_{[\text{km}]})$	$141.52+28 \cdot \log(d_{[\text{km}]})$
Shadowing de-correlation length	5 m	20 m

Table 2 Transport block size and bit rate associated to CQI

CQI	Modulation	Transport block size (bits)	R(CQI) (kbps)
CQI 5	QPSK	377	188.5
CQI 8	QPSK	396	198.0
CQI 15	QPSK	663.8	331.9
CQI 22	16-QAM	1433.6	716.8

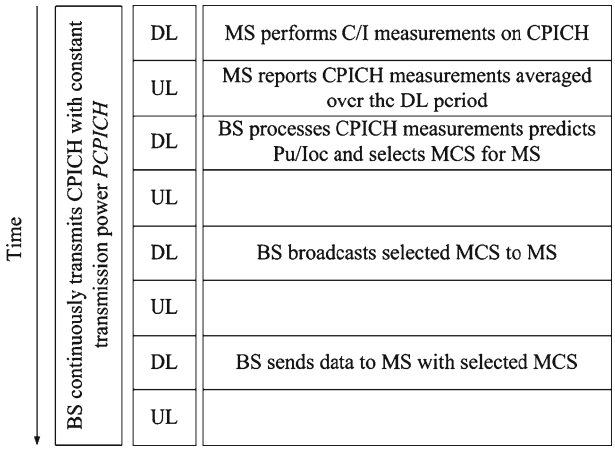

Fig. 3 Channel Quality measurements and MCS selection cycle

2. A CQI identifier is selected according to the link adaptation algorithm, using the available CQI options from the physical layer;
3. An idle ARQ channel j is selected to hold and manage the ARQ transmission;
4. The packet is transmitted and received at the MS. Soft retransmissions are combined with previous packet transmissions (chase combining) and the ARQ messages are generated accordingly. These messages are then signalled to the BS, and the ARQ processes are released if the messages are positive Acknowledgements (ACKs).

Figure 3 illustrates the mechanism used to sense the CQI over the various frequency bands. The sensing is based on quality measurements of the Common Pilot Channel (CPICH) performed by the MS. In fact, the MS performs a prediction of the ratio between the received power and the received inter-cell interference. Several approaches may be followed.

The MS can be either in the active or passive mode. In the active mode, the user is continuously measuring the received CQI over both frequencies. In the passive mode, the measurements are periodically sent to the Radio Network Controller (RNC). The CQI measurements are communicated to the HSDPA RNC through the High-Speed Dedicated Physical Control Channel (HS-DPCCS). Although the active mode has the advantage of self-detection, allowing for an aggressive exploitation of radio channel capacity, the passive mode may be preferred when the purpose is energy saving at the MS and reduced signalling overhead. If no transmission has been previously attempted in a given band, the best CQI is optimistically assumed. Instead, if a transmission has already occurred, the value for the CQI is calculated from the average of the last transmissions within a given period, i.e., moving average calculation.

3 General Multi-Band Scheduling

SA offers an added dimension for user scheduling and poses an optimisation problem for the best network resource exploitation. The scheduling problem can be formulated as a General Assignment Problem [23]. In this specific scenario, the user allocation problem is referred to

as GMBS. The proposed Profit Function (PF) maximises the total throughput of the operator via a single objective problem.[1]

The GMBS problem can be solved with IP. The GMBS PF is defined considering the ratio between the rate available on a single Downlink (DL) channel and the requested rate by the service flow and is expressed as follows:

$$\text{(PF)} \quad \sum_{b=1}^{m} \sum_{u=1}^{n} W_{bu} x_{bu} \tag{2}$$

where x_{bu} is the allocation variable and the normalised metric W_{bu} is given by:

$$W_{bu} = \frac{[1 - PER(CQI_{bu})] \cdot R(CQI_{bu})}{S_{\text{rate}}} \tag{3}$$

where S_{rate} is the NRTV service rate, PER(CQI$_{bu}$) is the average Packet Error Rate (PER) occurred in previous transmissions that the DL channel for user u on band b is suffering for the Modulation and Coding Scheme (MCS) supported (0 in the case no transmissions has ever occurred), and R(CQI$_{bu}$) is the DL channel throughput for user u on band b, as a function of the MCS supported.

The constraints for GMBS vary, depending on the ability of the MSs to simultaneously transmit and receive in multiple frequencies (multiple transceivers at the MS), or just over a single band at the time. HSDPA physical layer [26] provides a set of orthogonal codes available for data transmission within a sub-frame. Codes may be allocated to service flows/users[2] in a flexible manner. More than one code can be assigned to a single user or a single code can be assigned to more than one user. The users on the same code adopt a time-division multiple-access which is managed by the packet scheduler. The allocation variable x_{bu} reflects the code allocation per users and is either a boolean value in the case of single code allocation, or a positive integer, $x_{bu} \in \{0, 1, \ldots, \max(N_{\text{codes}})\}$, in the case of multi-code allocation.

An example of multi-code allocation is shown in Fig. 4, where a RR packet scheduler is used in which all the users are satisfied within three TTIs. Two iterations of three TTIs are presented: user 1, allocated to band 1, has $x_{1\,1} = 5$, while user 14, allocated to band 2, has $x_{2\,14} = 3$.

In the following explanation, a single-frequency single-code allocation will be explored with a RR scheduler. The RR scheduler was selected since it is the one with least interference on upper layer algorithms.[3]

In single-frequency single-code allocation, the GMBS presents the following constraints:

1. Allocation Constraint (AC): each user can be allocated only to a single frequency band with a single orthogonal code:

$$\text{(AC)} \quad \sum_{b=1}^{m} x_{bu} \leq 1, \qquad x_{bu} \in \{0, 1\} \quad \forall u \in \{0, \ldots, n\} \tag{4}$$

[1] However, multiple objectives can be easily introduced, as in [24], with a Multiple Objectives GAP (MO-GAP). Several objectives, such as fairness and QoE requirements, can be included via a linear combination, also referred to as "scalarization" [25].

[2] Each user in the network is assumed to bear only one service flow. With this assumption, the terms service flow and user can be used interchangeably.

[3] For instance, in the case of a maximum C/I scheduler, the users with worst channel conditions would not have been served and the full extent of the proposed algorithm would not be thoroughly revealed.

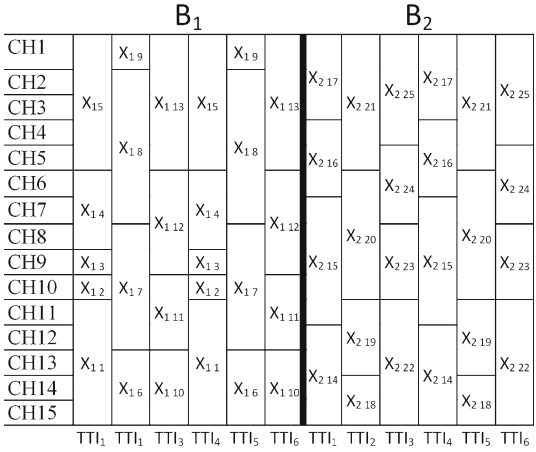

Fig. 4 Allocation matrix example over two frequency bands

b \ u	1	2	3	...	n
1	1	0	1	...	0
2	0	1	0	...	0
3	0	0	0	...	0
⋮	⋮	⋮	⋮	...	⋮
m	0	0	0	....	0
↓	↓	↓	↓	↓	↓
$\sum_b x_{bu}$	1	1	1	1	1

Fig. 5 Example of an allocation matrix X for single-frequency single-code GMBS

2. Bandwidth Constraint (BC): the total number of users on each band is upper bounded by the maximum normalised load that can be handled in the band, $L_b^{\max} \in [0, 1]$:

$$\text{(BC)} \quad \sum_{u=1}^{n} \frac{S_{\text{rate}} \cdot (1 + R_{Tx} \cdot \text{PER}(\text{CQI}_{bu}))}{R(\text{CQI}_{bu}) \cdot N_{\text{codes}}} \cdot x_{bu} \leq L_b^{\max} \quad \forall b \in \{1, \ldots, m\} \tag{5}$$

where the first term is the requested service data rate for user u, including the packet loss, normalized with the maximum data rate that the network can offer to the user u on band b which is $R(\text{CQI}_{bu}) \times N_{\text{codes}}$ where N_{codes} is the maximum number of parallel codes available in HSDPA. $R_{Tx} = 2$ is the number of H-ARQ retransmissions. BC accounts for the user traffic requirement, DL capacity and overhead caused by packets lost. The load constraint for each band, $L_b^{\max}$, is lower than one because of the padding caused when the packets from upper layers are fragmented to fit the MAC Packet Data Unit (MPDU), and signalling overhead.

Figure 5 presents one example, for a given case, for the allocation matrix $X = [x_{bu}]$, with $b = \{1, \ldots, m\}$ and $u = \{1, \ldots, n\}$. With two bands, $m = 2$ and $L^{\max} = \left[L_1^{\max},\ L_2^{\max}\right]^T$.

After several tests performed to find the best load threshold, a load factor of 75% has been chosen. This value was found through extensive simulation. It is a parameter that should be tuned by the operator. To find an heuristic that outputs this parameter is out of the scope of this work.

4 Average SINR Analysis with Unitary Frequency Reuse Pattern

The SA gain has been evaluated for several inter-cell distances with a frequency reuse pattern one. In order to have comparable results, SA needs to be analysed at constant average SINR. To obtain the average SINR, a method similar to the described in chapter 12 from [27] was applied. By tuning the BSs transmitter power, the average SINR was kept constant.

4.1 SINR at a Given Position

In general, given a BS transmitter power P_{Tx}, the MS SINR at a position (x, y) can be expressed as:

$$\mathrm{SINR}(P_{Tx}, x, y) = \frac{P_{\mathrm{ow}}(P_{Tx}, x, y)}{(1-\alpha)\cdot P_{\mathrm{ow}}(P_{Tx}, x, y) + P_{\mathrm{nh}}(P_{Tx}, x, y) + P_{\mathrm{noise}}} \tag{6}$$

where P_{noise} is thermal noise power, α is the orthogonality level of the codes [28], P_{ow} is the power received from the own cell, and P_{nh} is the total amount of interfering power coming from the neighbour cells (6 cells in the case of hexagonal cell deployment).

At 2 GHz, P_{ow} can be expressed as:

$$P_{\mathrm{ow}}(P_{Tx}, x, y) = P_{Tx} G_{Tx} G_{Rx} 10^{-\frac{128.1+37.6\cdot\log\sqrt{y^2+x^2}}{10}} \tag{7}$$

where G_{Tx} and G_{Rx} are the antenna gains.

P_{nh} is the interfering power received by a MS from the first ring of six neighbours cells, as illustrated in Fig. 6. It is given by:

$$P_{\mathrm{nh}}(P_{Tx}, x, y) = \sum_{i=1}^{6} I_i(P_{Tx}, x, y) \quad \text{with,} \quad I_1 = I_6,\ I_2 = I_5,\ I_3 = I_4 \tag{8}$$

where $I_i(P_{Tx}, x, y) = P_{Tx} G_{Tx} G_{Rx} 10^{-\frac{\mathrm{PL}(x,y)^i}{10}}$ and the following functions for the path loss, PL, at 2 GHz band stand as:

$$\begin{aligned}
\mathrm{PL}(x, y)^{1,6} &= 128.1 + 37.6\cdot\log\sqrt{\left(\frac{3}{2}R - x\right)^2 + \left(\frac{\sqrt{3}}{2}R\right)^2} \\
\mathrm{PL}(x, y)^{2,5} &= 128.1 + 37.6\cdot\log\sqrt{\left(\sqrt{3}R\right)^2 + x^2} \\
\mathrm{PL}(x, y)^{3,4} &= 128.1 + 37.6\cdot\log\sqrt{\left(\frac{3}{2}R + x\right)^2 + \left(\frac{\sqrt{3}}{2}R\right)^2}
\end{aligned} \tag{9}$$

The geometry symmetries have been considered and I_i is the i^{th} cell interference.

Figure 7 shows the variation of the SINR as a function of the MS-BS distance, d ($0 \leq d \leq R$). Results are presented for a cell radius of 300 and 1,500 m.

4.2 Average Cell SINR

The average SINR within a cell is the SINR measured by a MS with uniform probability density function for its deployment over the cell area. It depends on the cell radius, R, and on the BS transmitter power, P_{Tx}, as follows:

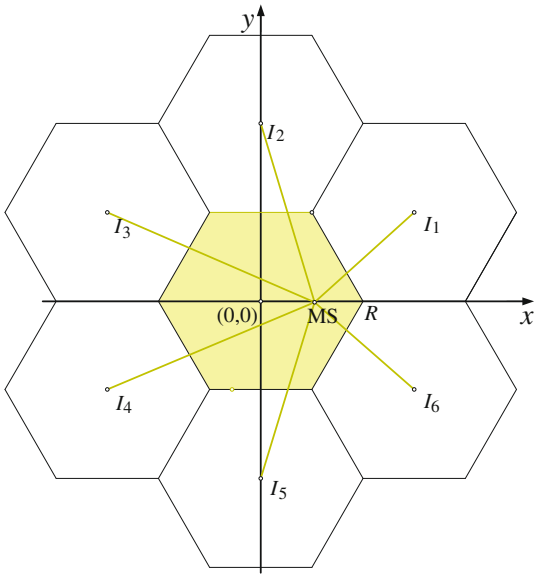

Fig. 6 Simulation topology of the HSDPA network

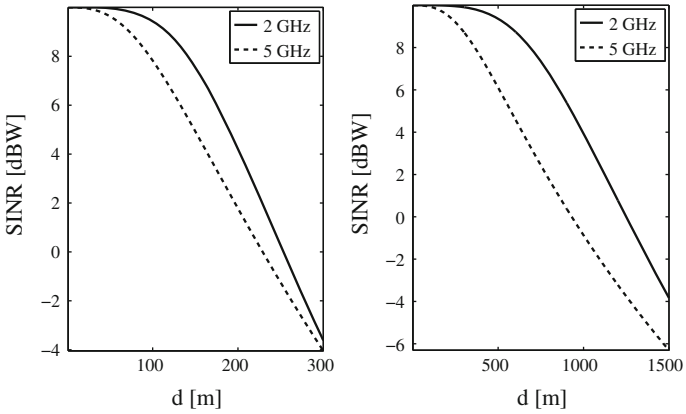

Fig. 7 From left to right, SINR as a function of the MS-BS distance for two cell radii ($R \in \{300,1,500\}$ m) and $P_{Tx} = 1$ dBW

$$\overline{\mathrm{SINR}}(R, P_{Tx}) = \frac{\overline{P}_{\mathrm{ow}}(R, P_{Tx})}{(1-\alpha)\overline{P}_{\mathrm{ow}}(R, P_{Tx}) + \overline{P}_{\mathrm{nh}}(R, P_{Tx}) + P_{\mathrm{noise}}} \tag{10}$$

where $\overline{P}_{\mathrm{nh}}(R, P_{Tx})$ is the average interference power from the six neighbouring cells. The average interference generated by a neighbour cell can be calculated by integrating each fraction of the interfering power over the area of the affected cell. Figure 8 shows one affected cell in the origin of the coordinates and one interfering cell, at (x_0, y_0). By integrating over the hexagonal cell area, the average level of received power from a neighbour cell $\bar{I}$ may be calculated as:

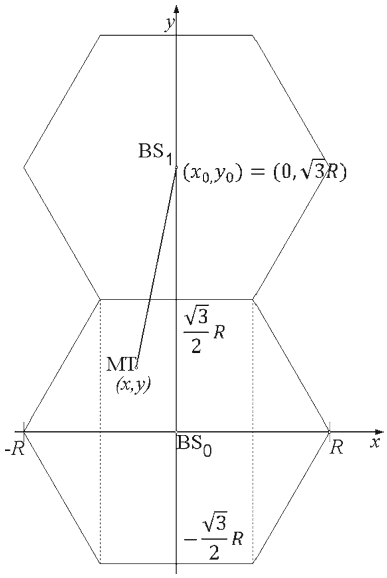

Fig. 8 Interference received from neighbouring cells

$$\bar{I}(R, P_{Tx}) = \int_y \int_x f_I(P_{Tx}, x, y)dxdy = \int_y \int_x \frac{P_{Tx}G_{Tx}G_{Rx}}{A_{Cell}}\text{PL}(x, y)dxdy \quad (11)$$

where A_{Cell} is the total affected cell area. $\overline{P}_{\text{nh}}(R, P_{Tx}) = 6 \cdot \bar{I}(R, P_{Tx})$ as the surrounding interfering neighbours are all at the same distance, $\sqrt{3}R$. The variation of the average received interference with the cell radius is shown in Fig. 17, in the Appendix. The details for the calculation of the average interference are also reported in the Appendix.

$\overline{P}_{\text{ow}}(R, P_{Tx})$ is the average signal power within a cell. It may be obtained following an approach similar to the one used for the average interference calculation, with a different integrand function, f_p, which, due to the geometry of the problem, has a simpler expression. The following integrand function is reported for the 2 GHz channel model:

$$f_{P_{\text{ow}}}(P_{Tx}, x, y) = \frac{P_{Tx}G_{Tx}G_{Rx}}{A_{\text{ow}}} 10^{-\frac{128.1+37.6\cdot\log\sqrt{y^2+x^2}}{10}} \quad (12)$$

A detailed calculation is reported in the Appendix and the results for the average power within the cell are shown in Fig. 17. The average SINR results are shown in Fig. 9. The average SINR at 5 GHz band decreases faster after 300 m, as it suffers higher pathloss effect. After 2,000 m, the network in the 5 GHz band starts to be noise-limited and the impact of interference is lower.

4.3 Transmitter Power Normalization Procedure

The goal of the Average SINR analysis is to determine a set of transmitting powers P_{Tx} in order to have a constant average SINR for all the cell radii. From (10), assuming the antenna gains are constant, the average SINR for a given radius, R_0, in the cell only depends on P_{Tx}.

In order to determine the values for the power that should be used at 2 and 5 GHz, we first found the transmitter power that corresponds to the maximum average SINR (with a difference lower than 0.01 dB to such a maximum) for $R_0 = 1{,}800$ m, P_{Tx,R_0}, in each of the

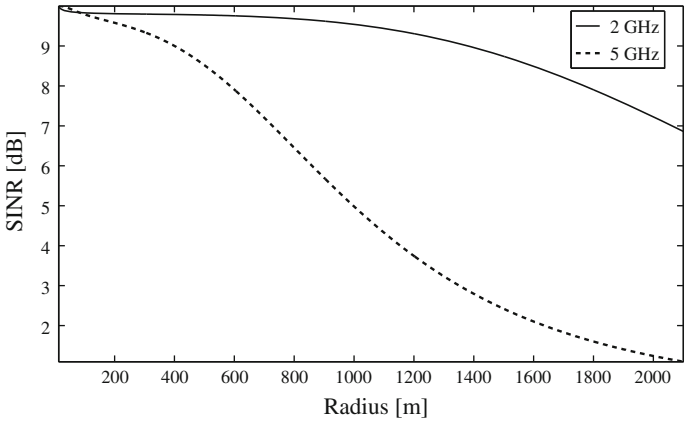

Fig. 9 Average SINR (dB) as a function of the cell radius in meters

Table 3 Values for the normalized transmitter power P_{Tx,R_0} (dBW), for the 2 and 5 GHz bands

Band	Radius (m)					
	300	600	900	1,200	1,500	1,800
2 GHz	−8.14	5.92	14.09	19.85	24.29	27.90
5 GHz	2.26	15.00	22.92	29.22	35.21	43.28

frequency bands. Then, for $R \in \{300, 600, 900, 1{,}200, 1{,}500, 1{,}800\}$ m, we found $P_{Tx,R}$ such that:

$$\overline{\text{SINR}}(R, P_{Tx}) = \overline{\text{SINR}}(R_0, P_{Tx,R_0}) \tag{13}$$

which provided the values for the transmitter power presented in Table 3, for the selected values of the cell radius. As these values for the power correspond to the maximum average SINR, the 5 GHz band non-covered area was kept to the minimum, less than 0.88% for $R \geq 600$ m and less than 1.08% for $0 < R \leq 600$ m.

5 Results

The performance of the SA user allocation is assessed by using the total Service Throughput (ST) metric, which is the total number of bits that have been transmitted and correctly received by all the users in the cell:

$$\text{ST}_{[\text{bits}/s]} = \frac{b_{\text{serv}}(p)}{k \cdot T} \tag{14}$$

where $b_{\text{serv}}(p)$ is the number of bits received in a given period p, T is the transmit time interval, and $k \cdot T$ is the total simulation time. Users are deployed on the cell with an uniform spatial distribution, within the cell radius R. Simulations were performed by considering the set of cell radii $R = \{300, 600, 900, 1{,}200, 1{,}500, 1{,}800\}$ m, with overlapping 2 and 5 GHz bands coverage, as shown in Fig. 2. The NRTV calls are modelled by a Poisson distribution, and the call duration is exponentially distributed with an average of 180 s. The 95% confidence interval is represented in the curves by the vertical bars.

Figure 10 reports the total ST for a system without iCRRM, using the standard CRRM from [18]. In such system, each one of the two frequency bands are managed separately.

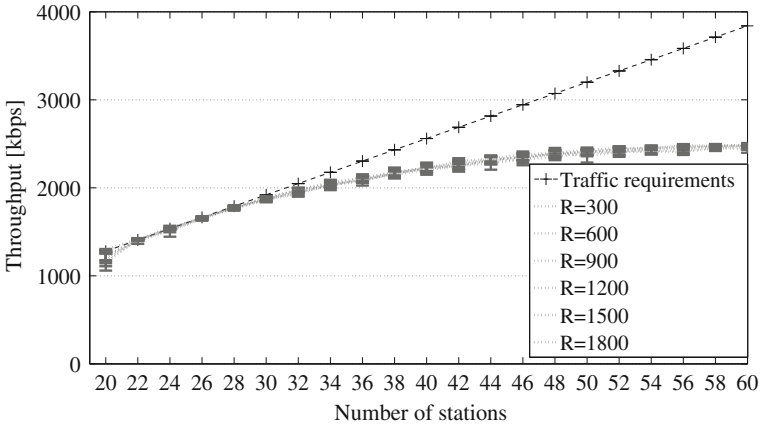

Fig. 10 Average throughputs without the iCRRM

NRTV session requests are expressly assigned to one of the two bands and it is not possible to switch a session from one band to the other. The results show approximately the same network capacity for variable cell radius. The ST reported in Fig. 10 is the sum of the service throughput in both frequency bands, 2 and 5 GHz. The traffic requirement is the traffic needed to satisfy all the users (i.e., the NRTV required data rate, times the number of users in the system).

The system can achieve better performance if MSs are allowed to be switched between bands. Figure 11 shows the results in the presence of the iCRRM with the GMBS algorithm proposed in Sect. 3, for several cell radii with normalized power. Due to the power normalization procedure, the performance of the iCRRM is almost constant for all the cell radii. In the saturation point which is located around 60 active MSs, for $R = 1,500$ m, the total throughput increases from 2430 kbps to 3170 kbps: a gain of 30% is achieved compared to the absence of iCRRM. Figure 12 presents the throughput gain in percentage and the absolute gain as a function of the cell radius under a constant average SINR: the power normalization procedure proposed in the previous section allows for fair results comparison with variable

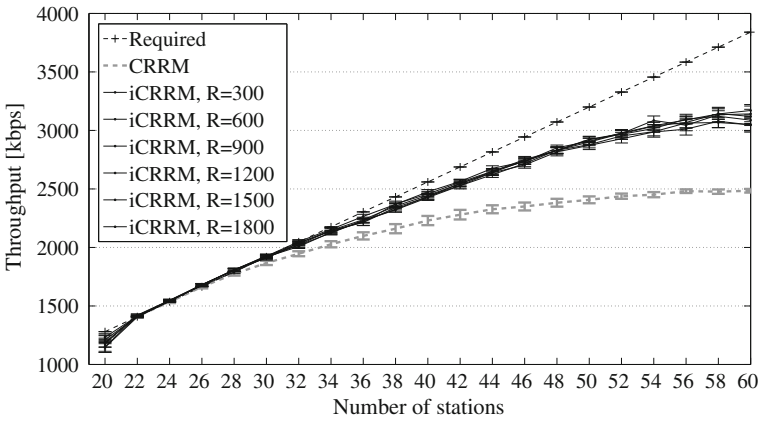

Fig. 11 Average service throughput with the iCRRM with normalized power

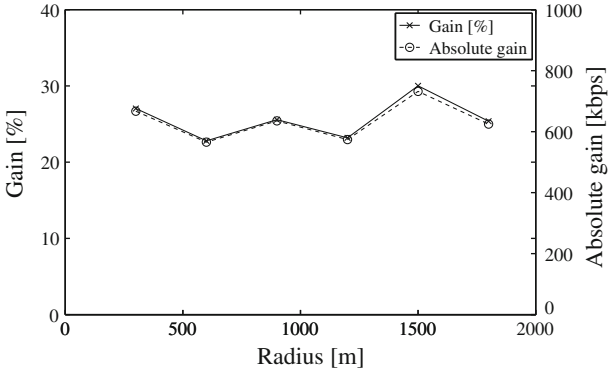

Fig. 12 Gain between the presence and absence of the iCRRM as a function of the cell radius for 60 users

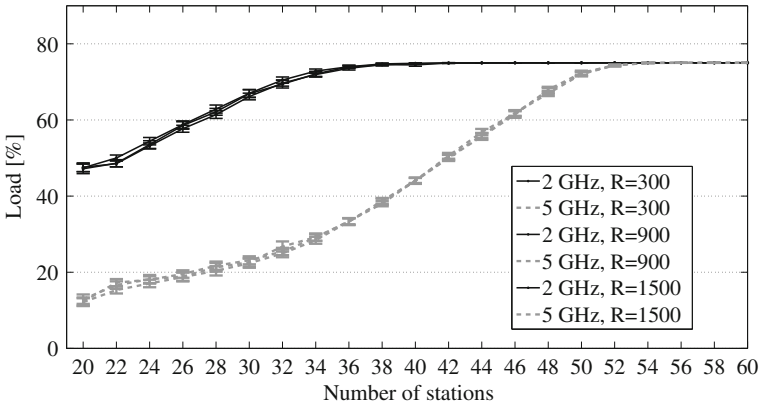

Fig. 13 Variation of the load with the number of stations for both frequency bands for $R = 300$, 900 and 1,500 m

cell radius. The almost constant gain demonstrates the potentiality of iCRRM over a wide range of cell coverage distances.

Figure 13 shows the load variation depending on the number of active MSs in the cell for both frequency bands and $R = 300$, 900 and 1,500 m. Since the path loss is lower at 2 GHz compared to the 5 GHz band, in the case of low cell load, the iCRRM entity will mainly allocate the MSs to the 2 GHz band. Furthermore, the load management interventions are not frequent, as it is evident in Fig. 14 for the group of 20–29 users. As the load raises, the bandwidth constraint for the 2 GHz band becomes stringent and the iCRRM entity optimises the use of resources with more frequent MS switching between bands. Both bands have a higher throughput due to the switching of the user between the two bands, based on their respective channel qualities. When the system gets close to the load threshold level, both bands are equally populated with allocated MSs.

As the signalling overhead arising from SA may be an issue, it is worth analysing the number of frequency band exchanges that result from SA. Figure 14 presents the average number of exchanges, among simulations, as a function of the MS-BS distance with the

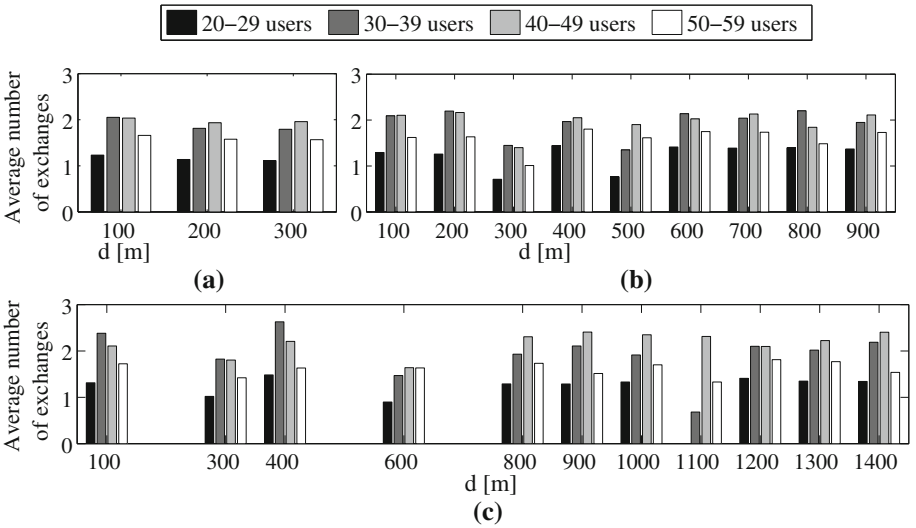

Fig. 14 Exchanges between frequency bands for cell radii **a** $R = 300$, **b** $R = 900$ and **c** $R = 1{,}500$ m

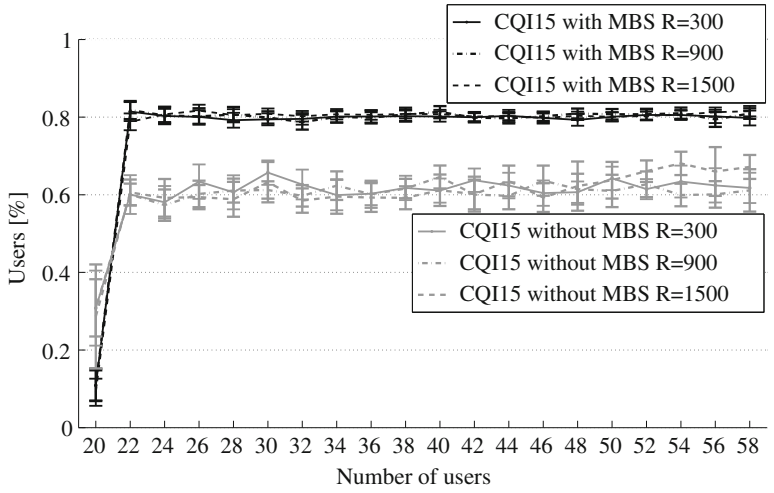

Fig. 15 CQI15 usage for cell radii $R = 300$, 900 and 1,500 m

number of active MSs as parameter. The MS-BS distance varies up to the cell radius R. Values are presented in different charts for a cell radius of $R = 300$, 900 and 1,500 m. The number of the iCRRM interventions is higher for medium loaded systems and it is lower when the active MSs are in the range of 20–29 and 50–59. Furthermore, the number of MSs switched between bands grows with the cell radius.

The two input parameters to the GMBS problem are analysed in Figs. 15 and 16. Figure 15 presents the percentage of users that use CQI15, one of the four MCSs available in the HSDPA system for $R = 300$, 900, 1,500 m. CQI15 is the one presented as it is dominant in the absence and presence of the iCRRM. However, when using iCRRM the set of MSs using CQI15 increases 20%. This is directly related to the capacity gain plotted in Fig. 12.

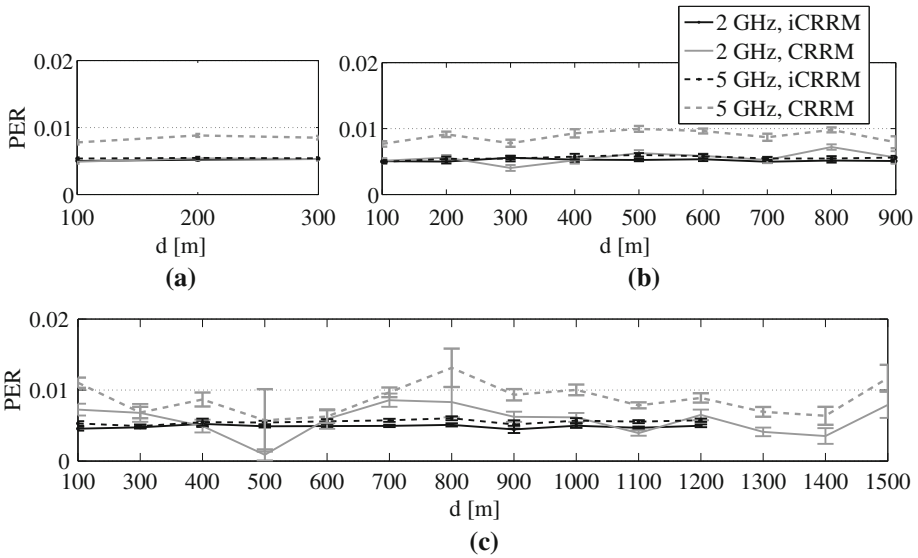

Fig. 16 PER variation for cell radii **a** $R = 300$, **b** $R = 900$ and **c** $R = 1{,}500$ m

Figure 16 presents the average PER as a function of the MS-BS distance for three cell radii: $R = 300$, 900 and 1,500 m; the use of iCRRM shows a significant reduction of PER, especially for the 5 GHz band. For all the cell radii, the GMBS is able to reduce the PER from 0.01 to 0.005 via an accurate selection of the MSs to be moved between 2 and 5 GHz, based on their channel quality in each frequency band.

6 Conclusions

This paper proposes an Integrated CRRM entity that has control over a pool of frequency resources. It assigns these resources to the active Mobile Stations with the solution of an optimisation problem with the objective of total Service Throughput maximisation. The proposal is in the scope of currently on-going work within the ITU-R towards International Mobile Telecommunications-Advanced systems, and in particular the use of Spectrum Aggregation. The hypotheses of the paper consider that Spectrum Aggregation can be successfully combined with Radio Resource Management techniques for an optimised performance.

In order to test the Integrated CRRM with several cell radii with comparable conditions, a formulation was developed that gives the average SINR in the cell considering frequency reuse pattern one. The transmitter powers were obtained for different cell radii in order to achieve a constant average SINR for variable cell radius and derive comparable results for iCRRM performance evaluation.

At the load saturation point, the iCRRM system has shown a gain of 23 up to 30%, compared to a system where the allocated Mobile Station cannot be switched between bands and the system cannot opportunisticaly exploit the variable channel qualities of the Mobile Stations.

With Integrated CRRM, the intra-operator Spectrum Aggregation procedure is able to support a higher number of Near Real Time Video users, due to the ability of scheduling their traffic according to the radio channel quality in different parts of the radio spectrum.

The achieved improvement is relative to scenarios where users are uniformly deployed on the cell.

Future work will analyse the impact of the spatial distribution of the users over the cell and the consideration of multi-service scenario. In this work, the General Multi-Band Scheduling Profit Function is based on the total throughput. Quality of Service requirements will be also included, in a scheduling problem with a linear combination of multiple objectives (scalarisation). A combined solution integrating the packet and the spectrum schedulers is foreseen to be able to greatly reduce the average delays and jitters, which are parameters of paramount importance for real-time services. Mobility patterns will also be analysed, showing the effectiveness of an Integrated CRRM to counter-fight shadowing in the support of the aforementioned real-time services and applications.

Acknowledgments The authors would like to acknowledge the support to the grants: Marie Curie European Reintegration Grant PLANOPTI (FP7-PEOPLE-2009-RG), Marie Curie Intra-European Fellowship OPTIMOBILE (FP7-PEOPLE-2007-2-1-IEF), to the FCT Ph.D. grant SFRH/BD/28517/2006; to UBIQUIMESH (PTDC/EEA-TEL/105472/2008) project and to OPPORTUNISTIC-CR (PTDC/EEA-TEL/115981/2009) project.

Appendix: Cellular Analysis for Constant Average SINR

In this appendix, detailed calculations of the average SINR are presented for various cell radii, in a cellular network of BSs with reuse pattern one. First, the average interference from a neighbour cell is presented. Then, the average signal power in the central cell is calculated in order to derive the SINR as function of the cell radius and transmit power.

The average interference from one neighbour cell is obtained, referring to the coordinate system in Fig. 8, as:

$$\bar{I}(R, P_{Tx}) = \int_x \int_y f_I(P_{Tx}, x, y)dydx = \int_x \int_y \frac{P_{Tx}G_{Tx}G_{Rx}}{A_{Cell}}\text{PL}(x, y)dydx \qquad (15)$$

where the area for an hexagonal cell is $A_{Cell} = \frac{3}{2}\sqrt{3}R^2$, the PL follows the models specified in Table 1, the distance being determined by $d = \sqrt{(y - y_0)^2 + (x - x_0)^2}$; $P_{Tx} = 1$ dBW, $G_{Tx} = 14$ dBi and $G_{Rx} = 0$ dBi. Figure 8 shows the division of the central hexagonal cell into three sub-regions (Fig. 17). Assuming $x_0 = 0$, $y_0 = \sqrt{3}R$, we may calculate the average interference as:

$$\bar{I}(R, P_{Tx}) = \sum_{r=1}^{3} \int_{\Gamma_x^r} \int_{\Gamma_y^r} f_I(P_{Tx}, x, y)dydx \qquad (16)$$

where the integration regions are as follows:

$$\Gamma_x^r = \left\{ \left[-R, -\frac{R}{2}\right], \left[-\frac{R}{2}, \frac{R}{2}\right], \left[\frac{R}{2}, R\right] \right\}$$

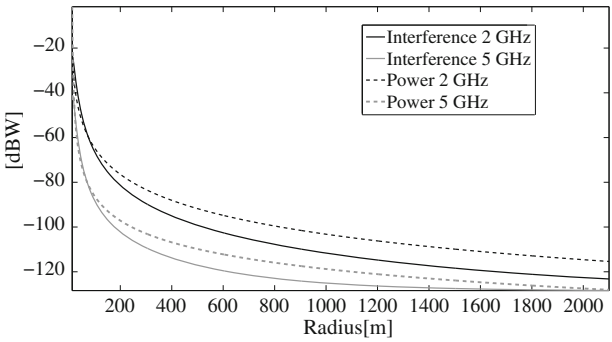

Fig. 17 Average power and interference (dBW) within a cell as a function of the inter-cell distance (m) with P_{Tx} 1 dBW

and

$$\Gamma_y^r = \left\{ \left[-\sqrt{3}x - \sqrt{3}R, \sqrt{3}x + \sqrt{3}R \right], \left[-\frac{\sqrt{3}}{2}R, \frac{\sqrt{3}}{2}R \right], \left[\sqrt{3}x - \sqrt{3}R, -\sqrt{3}x + \sqrt{3}R \right] \right\}$$

For the 2 GHz band, $f_I(P_{Tx}, x, y)$ is given by:

$$f_I(P_{Tx}, x, y) = \frac{P_{Tx} G_{Tx} G_{Rx}}{A_{\text{cell}}} 10^{-\frac{128.1+37.6 \cdot \log\sqrt{(y-\sqrt{3}R)^2+x^2}}{10}} \tag{17}$$

As R is positive (16) is solvable. Then:

$$\int_{\Gamma_{x,y}^r} f_I(P_{Tx}, x, y) dy dx = P_{Tx} G_{Tx} G_{Rx} \cdot 10^{-\frac{\sum_{r=1}^{3} \int_{\Gamma_{x,y}^r} \left(128.1+37.6 \cdot \log\sqrt{(y-\sqrt{3}R)^2+x^2}\right) dy dx}{10 \cdot A_{\text{cell}}}} \tag{18}$$

Considering that the distance in the path loss equation is expressed in kilometres and that:

$$\int_{\Gamma_{x,y}^1} dy dx = \frac{\sqrt{3}}{4} R^2 \tag{19}$$

the steps for solving the integral in the second term of (18) over the region $\Gamma_{x,y}^1$ are as follows:

$$\int\limits_{\Gamma^1_{x,y}} \left(128.1 + 37.6 \cdot \log\sqrt{(y-\sqrt{3}R)^2 + x^2}\right) dydx$$
$$= \frac{37.6}{2} \int\limits_{\Gamma^1_{x,y}} \log\left[\left(y-\sqrt{3}R\right)^2 + x^2\right] dydx$$
$$+(128.1 - 37.6 \cdot \log(1000))\frac{\sqrt{3}}{4}R^2. \tag{20}$$

The solution for the integral in the second term of (20) is:

$$\int\limits_{\Gamma^1_{x,y}} \log\left[\left(y-\sqrt{3}R\right)^2 + x^2\right] dydx = \int\limits_{\Gamma^1_{x,y}} \frac{\ln\left[\left(y-\sqrt{3}R\right)^2 + x^2\right]}{\ln(10)} dydx$$
$$= \ln(10)^{-1} \int\limits_{\Gamma^1_x} \left(-4\sqrt{3}R - 4\sqrt{3}x + \frac{2Rx}{3} + 2x \cdot \arctan\left[\frac{\sqrt{3}(2R+x)}{x}\right]\right.$$
$$+\sqrt{3}x \cdot \ln\left(4x^2\right) + 2\sqrt{3}R \cdot \ln\left[4\left(3R^2 + 3Rx + x^2\right)\right]$$
$$\left.+\sqrt{3}x \cdot \ln\left[4\left(3R^2 + 3Rx + x^2\right)\right]\right) dx. \tag{21}$$

The average interference power can be obtained with the evaluation of a linear combination of the integrals of arctan, ln and polynomial functions. The integration over region $\Gamma^2_{y,x}$, by applying the method of integration by parts, is simple to obtain. Over region $\Gamma^3_{y,x}$, the steps to be followed are similar to the ones outlined in (19), (20) and (21). The average interference that comes from each of the surrounding cells is equal as the interfering BS is always at the same distance $\sqrt{3}R$ from the central cell, see Fig. 6.

The average signal power in the intended cell can be calculated with the same approach used for the average interference power, substituting the integrand function f_I with f_P, which is reported for the 2 GHz as follows:

$$f_P(P_{Tx}, x, y) = \frac{P_{Tx}G_{Tx}G_{Rx}}{A_{\text{ow}}} 10^{-\frac{128.1+37.6\cdot\log\sqrt{y^2+x^2}}{10}} \tag{22}$$

The average power is calculated as:

$$\overline{P}_{\text{ow}}(R, P_{Tx}) = \sum_{r=1}^{6} \int\limits_{\Gamma^r_x} \int\limits_{\Gamma^r_y} f_P(P_{Tx}, x, y) dydx \tag{23}$$

where

$$\Gamma^r_x = \left\{\left[-R, -\frac{R}{2}\right], \left[-\frac{R}{2}, -Fr\right], [-Fr, Fr], [-Fr, Fr], \left[Fr, \frac{R}{2}\right], \left[\frac{R}{2}, R\right]\right\}$$

and

$$\Gamma_y^r = \left\{ \left[-\sqrt{3}x - \sqrt{3}R, \sqrt{3}x + \sqrt{3}R \right], \left[-\frac{\sqrt{3}}{2}R, \frac{\sqrt{3}}{2}R \right], \left[-\frac{\sqrt{3}}{2}R, -Fr \right], \left[Fr, \frac{\sqrt{3}}{2}R \right], \left[-\frac{\sqrt{3}}{2}R, \frac{\sqrt{3}}{2}R \right], \left[\sqrt{3}x - \sqrt{3}R, -\sqrt{3}x + \sqrt{3}R \right] \right\}$$

Equation (23) is unsolvable if the integration region includes $(x, y) = (0, 0)$ (where the BS is located). We adopted an approximation of the Fraunhofer distance, F_r, for an antenna radiator equal to 72 cm. If $R > F_r$ the integral is solvable. With a square approximation of the Fraunhofer region centered in (0,0), the total integration area is $A_{\text{ow}} = \frac{3}{2}\sqrt{3}R^2 - F_r^2$.

The average power calculation can thus be expressed as:

$$\int\limits_{\Gamma_{x,y}^r} f_P(P_{Tx}, x, y)dydx = P_{Tx}G_{Tx}G_{Rx} \cdot 10^{-\frac{\sum_{r=1}^{6} \int_{\Gamma_{x,y}^r} \left(128.1 + 37.6 \cdot \log\sqrt{y^2+x^2}\right)dydx}{10 \cdot A_{\text{ow}}}} \tag{24}$$

From all the integration regions in (24) the most complicated integrals to solve are the ones for $r = 1$ and $r = 6$. As their resolutions are similar, we outline the one for $r = 6$. Considering that the distance in the path loss is expressed in kilometres, and that:

$$\int\limits_{\Gamma_{x,y}^6} dydx = \frac{\sqrt{3}}{4}R^2 \tag{25}$$

then:

$$\begin{aligned} &\int\limits_{\Gamma_{x,y}^6} \left(128.1 + 37.6 \cdot \log\sqrt{y^2 + x^2}\right) dydx \\ &\quad = \frac{37.6}{2} \int\limits_{\Gamma_{x,y}^6} \log(y^2 + x^2)dydx + (128.1 - 37.6 \cdot \log(1000))\frac{\sqrt{3}}{4}R^2 \end{aligned} \tag{26}$$

The solution to the integral in the second term in (26) is given by:

$$\begin{aligned} &\int\limits_{\Gamma_{x,y}^6} \log(y^2 + x^2)dydx = \int\limits_{\Gamma_{x,y}^6} \frac{\ln(y^2 + x^2)}{\ln(10)}dydx \\ &\quad = \ln(10)^{-1} \int\limits_{\Gamma_x^6} \left(2(-\sqrt{3}x + \sqrt{3}R) \ln\left[(-\sqrt{3}x + \sqrt{3}R)^2 + x^2 \right] \right. \\ &\qquad \left. - 4(-\sqrt{3}x + \sqrt{3}R) + 4x \cdot \arctan\left[\frac{-\sqrt{3}x + \sqrt{3}R}{x} \right] \right) dx. \end{aligned} \tag{27}$$

The second term of the last member of (27) it is a polynomial integration. The first and third terms of the last member of (27) are solved by using the method of integration by parts. The integration is shown for exemplification for the third term only:

$$\int \arctan\left[\frac{-\sqrt{3}x+\sqrt{3}R}{x}\right]dx$$
$$= 2x^2 \cdot \arctan\left[\frac{-\sqrt{3}x+\sqrt{3}R}{x}\right] + 2\sqrt{3}R\left[\frac{1}{4}x - \frac{3}{4}R\cdot\left(-\frac{1}{2\sqrt{3}}\cdot\arctan\left[\frac{-3R+4x}{\sqrt{3}R}\right] - \frac{1}{4}\cdot\ln\left(3R^2-6Rx+4x^2\right)\right)\right] \quad (28)$$

The second integration over regions $\Gamma^3_{x,y}$ and $\Gamma^4_{x,y}$ do not exist for $x = 0$. Dividing the region Γ^3_x (equal to Γ^4_x) into two subregions, $[-Fr, 0[$ and $]0, Fr]$, the integral can be put in the improper integral form and then solved by parts:

$$\int_{\Gamma^3_x}\int_{\Gamma^3_y} f_P(P_{Tx}, x, y)dydx$$
$$= \lim_{\epsilon\to 0^-}\int_{-Fr}^{\epsilon}\int_{\Gamma^3_y} f_P(P_{Tx}, x, y)dydx + \lim_{\epsilon\to 0^+}\int_{\epsilon}^{Fr}\int_{\Gamma^3_y} f_P(P_{Tx}, x, y)dydx \quad (29)$$

The average power can now be obtained for the whole hexagon, except in the square with the side length equal to the Fraunhofer distance and the average SINR in (10) can be finally calculated.

References

1. Key results of World Radiocommunication Conference (WRC-07). [Online]. Available: http://www.itu.int/dms_pub/itu-t/oth/21/04/T21040000030014PPTE.ppt.
2. Third Generation Partnership Project 3GPP. [Online]. Available: www.3gpp.org.
3. FP6 IST Project WINNER and WINNER II. [Online]. Available: www.ist-winner.org.
4. EU CELTIC Project WINNER+. [Online]. Available: http://projects.celtic-initiative.org/winner+/.
5. 3GPP TS 36.213 v9.0.0, Evolved Universal Terrestrial Radio Access (E-UTRA); Physical layer procedures (Release 9). (2009). *3rd Generation Partnership Project*. Technical Specification Group Radio Access Network December 2009.
6. 3GPP TR 36.814 v1.7.0, Further Advancements for E-UTRA Physical Layer Aspects (Release 9). (2010). *3rd Generation Partnership Project*. Technical Specification Group Radio Access Network, February 2010.
7. 3GPP TR 36.815 v9.0.0, LTE-Advanced feasibility studies in RAN WG4 (Release 9). (2010). *3rd Generation Partnership Project*. Technical Specification Group Radio Access Network, March 2010.
8. Chen, L., Chena, W., Zhang, X., & Yang, D. (2009). Analysis and simulation for spectrum aggregation in LTE-advanced system. In *Proceedings of the IEEE 69th Vehicular Technology Conference (VTC2009-Fall)* (pp. 1–6). USA: Anchorage.
9. Yuan, G., Zhang, X., Wang, W., & Yang, Y. (2010). Carrier aggregation for LTE-advanced mobile communication systems. *IEEE Communications Magazine, 48*(2), 88–93.
10. Wang, Y., Pedersen, K., Mogensen, P. & Sorensen T. (2009). Carrier load balancing methods with bursty traffic for LTE-Advanced systems. In *Proceedings of the IEEE International Symposium on Personal, Indoor and Mobile Radio Communications (PIMRC09)*, Tokyo, Japan.
11. Wang, Y., Pedersen, K., Sorensen, T., & Mogensen, P. (2010). Downlink Transmission in Multi-Carrier Systems with Reduced Feedback. In *Proceedings of the IEEE 70th Vehicular Technology Conference (VTC2010-Spring)*, Taipei, Taiwan.

12. Dixtona, J., Politis, C., & Wijting, C. (2008). Considerations in the choice of suitable spectrum for mobile communications. In *Proceedings of the Wireless World Research Forum Meeting 21*. Sweden: Stockholm.
13. Meucci, F., Cabral, O., Velez, F. J., Mihovska, A., & Prasad, N. R. (2009). Spectrum Aggregation with Multi-Band User Allocation over Two Frequency Bands. In *Proceedings of the IEEE Mobile WiMAX Symposium (MWS 2009)*. California, USA: Napa Valley.
14. (2007, March) *IST-4-027756 WINNERII D 5.10.2 Spectrum Requirements for System beyond IMT-2000*. [Online]. Available: http://www.ist-winner.org/deliverables.html.
15. Lee, W. C. Y. (1993). *Mobile communications, design fundamental* (2nd ed.). New York, NY: Wiley.
16. (2008, December) *EU CELTIC Project WINNER+, Deliverable 3.1, IMT-Advanced: Requirements and Evaluation Criteria*. [Online]. Available: http://projects.celtic-initiative.org/winner+/.
17. (2004) IST MATRICE-2001-32620, D4.5 Layer 2& 3 reference simulation results dynamic resource allocation algorithms and IP transport. September 2004, http://www.ist-matrice.org/.
18. Skehill, R., Barry, M., Kent, W., O'Callaghan, M., Gawley, N., & Mcgrath, S. (2007). The common RRM approach to admission control for converged heterogeneous wireless networks. *IEEE Wireless Communications Magazine, 14*(2), 48–56.
19. *Radio Resource Management Strategies, TR 25.922. 3GPP*. Technical Specification Group RAN, Working Group 2 (WG2).
20. 3GPP TR 25.892 v6.0.0, Feasibility Study for Orthogonal Frequency Division Multiplexing (OFDM) for UTRAN enhancement. (2004). *3rd Generation Partnership Project*. Technical Specification Group Radio Access Network, June 2004.
21. R1-03-0249, Validation of System-Level HSDPA Results for CDMA and OFDM in aFlat Fading Channel. (2003). *Nortel Networks*. 3GPP TSG-RAN-1 Meeting #31, 18–21 February 2003.
22. 3GPP2-C30-20030429-010, Effective SNR mapping for modelling frame error rates in multiple-state channels. Ericsson.
23. Karlof, J. K. (2005). *Integer programming: theory and practice* (1st ed), CRC.
24. Meucci, F., Mihovska, A., Anggorojati, B. & Prasad, N. R. (2008). Joint resource allocation and admission control mechanism for an OFDMA-based system. In *Proceedings of the 11th International Symposium on Wireless Personal Multimedia Communications (WPMC 2008)*. Finland: Lapland.
25. Kellerer, H., Pferschy, U., & Pisinger, D. (2005). *Knapsack problems*. Berlin: Springer.
26. TR25.211. (2005). *Physical channels and mapping of transport channels onto physical channels (FDD)*, 5th edn. 3GPP June 2005.
27. Chen, K.-C., Roberto, J., & Marca, B. (2008). *Mobile WiMAX* (1st ed.). West Sussex England: Wiley.
28. Holma, H., & Toskala, A. (2007). *WCDMA for UMTS—HSPA evolution and LTE* (1st ed.). West Sussex, England: Wiley.

Author Biographies

O. Cabral is a research assistant at Instituto de Telecomunicações, Universidade da Beira Interior, Covilhã, Portugal, where he has worked towards the Ph.D. degree since 2007. He recently submitted his final thesis work in the area of cognitive wireless communications. Orlando Cabral has been active in projects such as COST 2100 on Pervasive Mobile & Ambient Wireless Communications, the FCT funded project on Opportunistic Aggregation of Spectrum and Cognitive Radios: Consequences on Public Policies, and on Cross-Layer Optimization in Multiple Mesh Ubiquitous Networks. He has a number of publications as book chapters, peer-reviewed journals and international conferences.

F. Meucci was born in Prato, Florence, Italy, on November 1979. He received his M.S. degree in Electronic Engineering from the University of Florence, Italy in 2005. In 2004-2005 he has been working with the TIER group (Telecommunication Infrastructures for Emerging Regions) at the University of Berkeley, California. He received his Ph.D. in Telecommunications Engineering from the University of Florence in 2009. During 2008 and 2009, he has been with CTIF, Center for TeleInFrastruktur, Aalborg Denmark. From 2009 he is assistant researcher at LENST Laboratory in Florence focused on digital signal processing for MIMO OFDM. From 2010, he is also with Selex Galileo where he is responsible for the development of MIMO airborne radars. His main research areas are: OFDM, MIMO, MIMO radars, network capacity, cross layer design and spectrum management. He has recently published the book: "Single and Cross Layer MIMO Techniques for IMT-Advanced" with River Publisher, Denmark. He has founded the Florence Chapter and the Aalborg Chapter of Engineering without Borders in 2002 and 2009, respectively.

A. Mihovska has a Ph.D. in Mobile Communications from Aalborg University, Denmark, where she is an Associate Professor at the Center for TeleInfrastruktur (CTIF) at the Department of Electronic Systems. Since 2004, she has been involved in research and ITU standardisation activities working towards advanced radio system technologies for IMT-Advanced systems. In particular, she has been working on advanced radio resource management, cross-layer optimisation, and spectrum aggregation.

F. J. Velez (M'93-SM'05) received the Licenciado, M.Sc. and Ph.D. degrees in Electrical and Computer Engineering from Instituto Superior Tecnico, Technical University of Lisbon in 1993, 1996 and 2001, respectively. Since 1995 he has been with the Department of Electromechanical Engineering of Universidade da Beira Interior, Covilhã, Portugal, where he is Assistant Professor. He is also a researcher at Instituto de Telecomunicações, Lisbon, and was a Research Fellow in King's College London in 2008/09. He made or makes part of the teams of RACE/MBS, ACTS/SAMBA, COST 259, COST 273, COST 290, IST-SEACORN, IST-UNITE, PLANOPTI, COST 2100, COST IC0902 and COST IC0905 "TERRA" European projects, he participated in SEMENTE, SMART-CLOTHING and UBIQUIMESH Portuguese projects, and he was or is the coordinator of five Portuguese projects: SAMURAI, MULTIPLAN, CROSSNET, MobileMAN and OPPORTUNISTIC-CR. He is the coordinator of the WG2 (on Cognitive Radio/Software Defined Radio Coexistence Studies) of COST IC0905 "TERRA". Prof. Velez has authored two books, ten book chapters, around 100 papers and communications in international journals and conferences, plus 25 in national conferences, is a senior member of IEEE and Ordem dos Engenheiros (EUREL), and a member of IET and IAENG. His main research areas are cellular planning tools, traffic from mobility, cross-layer design, spectrum sharing/aggregation, and cost/revenue performance of advanced mobile communication systems.

N. R. Prasad IEEE Senior Member, is Associate Professor and head of research at the Center for TeleInfrastruktur (CTIF) at Aalborg University. She has over 14 years of management and research experience both in industry and academia. She has gained a large and strong experience into the administrative and project coordination of EU-funded and Industrial research projects. She joined Libertel (now Vodafone NL), The Netherlands in 1997. Till May 2001, she worked at Wireless LANs in Wireless Communications and Networking Division of Lucent Technologies, The Netherlands. From June 2001 to July 2003, she was with T-Mobile Netherlands, The Netherlands. Subsequently, from July 2003 to April 2004, at PCOM:I3, Aalborg, Denmark. She has been involved in a number of EU-funded R&D projects, including FP7 CIP-PSP LIFE 2.0, FP7 CIP-PSP ISISEMD, FP7 IP ASPIRE, FP7 IP FUTON, FP6 IP eSENSE, FP6 NoE CRUISE, FP6 IP MAGNET and FP6 IP Magnet Beyond as the latest ones. She is currently the project coordinator of the FP7 IST IP ASPIRE, FP7 CIP-PSP LIFE 2.0 and was project coordinator of FP6 NoE CRUISE. She was also the leader of EC Cluster for Mesh and Sensor Networks and is Counsellor of IEEE Student Branch, Aalborg. Her current research interests are in the area of SON, IoT, Identity Management, mobility, network management and monitoring; practical radio resource management; cognitive learning capabilities and modelling; Security, Privacy and Trust. Experience in other fields includes physical layer techniques, policy based management, short range communications. Her publications range from top journals, international conferences and chapters in books. She has also co-edited and co-authored two books titled "WLAN Systems and Wireless IP for Next Generation Communications" and "Wireless LANs and Wireless IP Security, Mobility, QoS and Mobile Network Integration", published by Artech House, 2001 and 2005. She is and has been in the organization and TPC member of international conferences.

R. Prasad has been holding the Professorial Chair of Wireless Information and Multimedia Communications at Aalborg University, Denmark (AAU) since June 1999. Since 2004 he is the Founding Director of the Center for TeleInfrastruktur (CTIF), established as large multi-area research center at the premises of Aalborg University. Ramjee Prasad is a Fellow of IEEE, the IET and IETE is a world-wide established scientist, which has given fundamental contributions towards development of wireless communications. He achieved fundamental results towards the development of CDMA and OFDM, taking the leading role by being the first in the world to publish books in the subjects of CDMA (1996) and OFDM (1999). He is the recipient of many international academic, industrial and governmental awards and distinctions of which the most recently is the cross of the order of chivalry (Ridderkorset af Dannebrogordenen) from the Danish Queen due internationalization of top-class telecommunication research and education. He has published a huge number of books (more than 25), journals and conferences publications (together more than 750), more than 15 patents, a sizeable amount of graduated Ph.D. students (over 60) and an even larger amount of graduated M.Sc. students (over 200). Several of his students are today worldwide telecommunication leaders themselves. He is the founding chairman of the Global ICT Standardization Forum for India (GISFI) and was the founding chairman of the European Center of Excellence in Telecommunications known as HERMES of which he is now the honorary chairman. Recently, under his initiative, international M.Sc. and Ph.D. programmes have been started with the Sinhgad Technical Education Society in India, the Bandung Institute of Technology in Indonesia and with the Athens Information Technology (AIT) in Greece.